

## CHAPTER 60

### EXPERIMENTS ON BED FORM GENERATION BY WAVE ACTION

by

G.R. Mogridge<sup>1</sup> and J.W. Kamphuis<sup>2</sup>

#### ABSTRACT

Experiments to determine the length, height and steepness of bed forms generated by wave action have been conducted in a laboratory wave flume and an oscillating water tunnel. The effects of a wide range of oscillatory flows were examined on polystyrene (specific gravity 1.05, diameter 1.54 mm), bakelite (specific gravity 1.60, diameter 0.52 mm), bakelite (specific gravity 1.51, diameter 0.67 mm) and sand (specific gravity 2.68, diameter 0.36 mm).

From the results of the experiments design curves were plotted which make it possible to predict the length and height of bed form that will develop on any specified sediment bed for given conditions of fluid oscillation.

#### INTRODUCTION

Knowledge about the formation of sand waves by wave action is limited when compared to what is known about sand waves caused by unidirectional flows. Yet bed forms resulting from wave action are at least as significant as those formed by unidirectional flows, since they exert an exceptionally strong influence on the sediment transport. For example, it is found in the laboratory wave flume that although sediment transport over a flat bed is in the same direction as the waves, i.e. the positive direction, when sand waves are present on the bed, the direction of net sediment transport may be either positive or negative. Therefore, as a first step to further research in sediment transport, a state of knowledge on sand waves should be reached where it is possible to predict what size sand waves form for specified sediment and wave conditions.

Different methods have been used to obtain data about the development of bed forms by the action of waves. Experiments have been conducted in laboratory wave flumes by

---

<sup>1</sup>Assistant Research Officer, Hydraulics Laboratory, National Research Council, Ottawa, K1A 0R6, Canada, formerly, Queen's University at Kingston, Canada.

<sup>2</sup>Associate Professor of Civil Engineering, Coastal Engineering Research Laboratory, Queen's University at Kingston, Canada.

Scott (9), Yalin and Russell (12), Kennedy and Falcon (6), Homma and Horikawa (3) and Horikawa and Watanabe (4). The range of bed form size that is obtainable beneath model waves is limited, however, and attempts have been made to extend this range by the use of prototype scale fluid motions. Thus, Bagnold (1) and Manohar (7) have studied bed forms using an oscillatory plate in still water. Carstens et al (2) studied the bed forms produced by the oscillatory flow generated in an oscillating water tunnel. Inman (5) actually measured the bed forms occurring in the ocean up to depths of 52 m and produced a valuable analysis of the data.

The present study commenced with wave flume experiments and was completed by extending the range of fluid amplitude and period of oscillation in an oscillating water tunnel. A number of wave flume experiments were repeated in the water tunnel to confirm that all experiments belonged to the same population.

#### DIMENSIONAL ANALYSIS

If  $Q$  is a quantitative property of the phenomenon of sand wave formation then it may be described by the following characteristic parameters,

$$Q = f_Q(\rho, \mu, U_m, a_\delta, D, \rho_s, g), \quad (1)$$

where  $\rho$  is the density and  $\mu$  the dynamic viscosity of the fluid;  $U_m$  is the maximum fluid velocity and  $a_\delta$  is the amplitude or semi-orbital diameter of the fluid motion, immediately outside the boundary layer.  $D$  is the median diameter and  $\rho_s$  is the density of the sediment. The acceleration due to gravity,  $g$ , is only necessary to describe the submerged weight of the sediment particle, i.e. it only appears in the submerged unit weight of the sediment, i.e.  $\gamma_s = (\rho_s - \rho) \cdot g$ . Therefore, equation 1 may be rewritten as,

$$Q = f'_Q(\rho, \mu, U_m, a_\delta, D, \rho_s, \gamma_s) \quad (2)$$

Dimensional analysis yields,

$$\pi_Q = \phi_Q \left( \frac{U_m D}{\nu}, \frac{\rho U_m^2}{\gamma_s D}, \frac{\rho_s}{\rho}, \frac{a_\delta}{D} \right), \quad (3)$$

where  $\nu = \mu/\rho$  is the kinematic viscosity of the fluid.

If the fluid motion is sinusoidal,

$$U_m = \text{constant} \left( \frac{a_\delta}{T} \right), \quad (4)$$

where  $T$  is the wave period and equation 3 may be simplified to,

$$\pi_Q = \phi_Q' \left( \frac{a_\delta D}{v T}, \frac{\rho a_\delta^2}{\gamma_S T^2 D}, \frac{\rho_S}{\rho}, \frac{a_\delta}{D} \right) \quad (5)$$

Because  $a_\delta$  is an important parameter in determining the bed form properties such as length and height, the variables as expressed in equation 5 are not convenient for design of the experimental procedure, since  $a_\delta$  occurs in three of the four variables. To simplify the experiments, equation 5 may be written as,

$$\pi_Q = \phi_Q'' \left[ \left( \frac{a_\delta \cdot D}{v \cdot T} \right)^2, \left( \frac{\gamma_S T^2 D}{\rho a_\delta^2} \right), \left( \frac{\rho a_\delta^2}{\gamma_S T^2 D} \right), \left( \frac{D}{a_\delta} \right)^2, \frac{\rho_S}{\rho}, \frac{a_\delta}{D} \right],$$

or

$$\pi_Q = \phi_Q'' \left( \frac{\gamma_S D^3}{\rho v^2}, \frac{\rho D}{\gamma_S T^2}, \frac{\rho_S}{\rho}, \frac{a_\delta}{D} \right) \quad (6)$$

As a result of mass transport, the fluid motion is rarely sinusoidal. The mass transport distance,  $\xi$ , the net distance moved by the fluid in a wave period immediately outside the boundary layer, is of minor importance in sand wave formation, and is small compared to  $2 \cdot a_\delta$ . During preliminary tests it was found to be difficult to exercise any control over its magnitude and therefore, instead of considering  $\xi$  as a separate parameter in equation 1, it was included with the fluid amplitude in a parameter called the effective fluid orbit length  $A$ , which is defined as,

$$A = 2 \cdot a_\delta + |\xi| \quad (7)$$

Thus the relationship finally used to describe the phenomenon becomes,

$$\pi_Q = \phi_Q''' \left( \frac{\gamma_S D^3}{\rho v^2}, \frac{\rho D}{\gamma_S T^2}, \frac{\rho_S}{\rho}, \frac{A}{D} \right), \quad (8)$$

which will be denoted as,

$$\pi_Q = \phi_Q'''(X_1, X_2, X_3, X_4),$$

where,

$$\begin{aligned} X_1 &= \frac{\gamma_s D^3}{\rho u^2} & ; & & X_2 &= \frac{\rho D}{\gamma_s T^2} \\ X_3 &= \rho s / \rho & ; & & X_4 &= \frac{A}{D} \end{aligned} \quad (9)$$

The effect of each of the above dimensionless variables on sand wave formation was obtained by organising the experiments so that the dimensionless bed form properties were measured for different values of  $X_4$ . The values of the remaining dimensionless variables were then altered one at a time in order to determine the effect of each individual variable on the bed form properties.  $X_1$  was varied by changing the temperature of the water,  $X_2$  was varied by altering the oscillation period,  $X_3$  was varied by using different sediments and in the wave flume  $X_4$  was varied by increasing the wave height or altering the water depth.

#### EXPERIMENTAL EQUIPMENT

Experiments were conducted at the Coastal Engineering Research Laboratory of Queen's University at Kingston. The wave flume experiments were performed in a 50 m long, 1 m wide and 1.2 m deep wave flume. Waves were absorbed by a porous beach. Wave reflections varied with the wave height and period, but reflection was generally less than 8%. The sediment bed was 6 m long, 1 m wide and 7.5 cm deep.

Since it is generally recognised (8), (10), that prototype bottom conditions are difficult to model accurately in a wave flume, such oscillatory motions were reproduced to prototype scale in an oscillating water tunnel. The tunnel has a working section 12 m long, 1 m deep and 0.5 m wide, Fig. 4, and is constructed of reinforced concrete. A detailed description of the design and construction of the tunnel is given by Riedel (8). The rear portion consists of a large chamber 2 m by 2 m in cross section in which a piston moves to oscillate the water. The piston is connected by means of a shaft which extends through the wall of the tunnel, to a crank arm which is driven by a 18.7 KW variable speed motor. The amplitude of the oscillation may be varied between 2.5 cm and 4 m by adjusting the eccentricity on the

crank arm, and the period of oscillation may be varied between 2.5 and 14 seconds by varying the speed of the motor.

For the present study, a false bottom was constructed in the tunnel for the purpose of placing a sediment bed which was 4 m long and 15 cm deep. Thus, the effective tunnel depth was 85 cm. Four different sediments were used; two crushed bakelite sediments, a sieved and washed natural sand and a polystyrene sediment. Their characteristics are given in Table I.

TABLE I  
Sediment Characteristics

<u>Sediment</u>	<u>Specific Gravity</u>	<u>Median Diameter D</u>	<u>Geometric Standard Deviation <math>\sigma_g</math></u>
Bakelite	1.60	0.52 mm	1.33
Bakelite	1.51	0.67 mm	1.40
Sand	2.68	0.36 mm	1.39
Polystyrene	1.05	1.54 mm	1.09

The geometric standard deviation was determined assuming a logarithmic normal distribution of sediment grain sizes. Thus, as an example, 68.2% of the grain sizes in the distribution are within the range  $D/\sigma_g$  to  $D \cdot \sigma_g$ .

The fluid orbit lengths in the vicinity of the bed forms were measured by recording the paths of almost neutrally buoyant particles in the fluid on videotape. A General Electric television camera fitted with a 15-150 mm zoom lens was used in conjunction with a television monitor and an International Video Corporation video-recorder with facility for slow motion playback. By replaying the videotape and following the tracer particles on the television monitor, accurate measurement of the fluid orbit length could be made. Bed form lengths and heights were measured on the glass windows.

#### EXPERIMENTAL RESULTS

##### (a) Variation of $X_4 = A/D$

Figures 1 and 2 show how, for some typical tests, the bed form length and height vary with  $X_4$  while the values of  $X_1$ ,  $X_2$  and  $X_3$  are kept constant. Figure 1 indicates for bed form length that at low values of  $X_4$ , the data falls on a straight line of slope 1:1. This means that,

$$\lambda = \text{constant} \cdot A,$$

and thus, the bed form length is independent of the sediment grain size and is a function of the fluid orbit length only. At high values of  $X_4$  in Fig. 1, the relationship becomes a horizontal straight line, i.e.

$$\Lambda = \text{constant} \cdot D$$

The constant of proportionality is a function of  $X_2$ .

The curves in Fig. 2 show that bed form height increases to a maximum as  $X_4$  increases and then begins to decrease to the stage where the height is barely measurable. The slope of the rising leg of the curve is slightly greater than 1:1 indicating that for this range of  $X_4$ , the bed form height depends largely on the fluid orbit length  $\Lambda$ , but also is slightly dependent on the grain size  $D$ . Thus, the bed form is slightly dependent on the shear stress exerted by the fluid on the sediment particles.

Figure 3 shows the effect of  $X_4$  on bed form steepness  $S$ , which is defined as bed form height divided by length. As  $X_4$  increases, the steepness increases to a maximum and then decreases.

Previous studies on bed forms resulting from wave action have produced results showing variation of  $\Lambda/D$  and  $\Delta/D$  with  $X_4$ , very similar to those in Figs. 1 and 2. Bagnold (1) using an oscillatory bed in still water and Carstens et al (2), using an oscillating water tunnel, both showed that the bed form length becomes dependent only on grain size diameter for high values of  $X_4$ . Bagnold (1), Carstens et al (2) and Yalin (12), all give curves for bed form height which reach a maximum and then continuously decrease for increasing fluid orbit lengths.

It may be concluded from the results that bed form properties such as length, height and steepness are in general strongly dependent on the fluid orbit length. Therefore, the experimental results to determine the effects of  $X_1$ ,  $X_2$ , and  $X_3$  are all plotted on graphs of dimensionless bed form property against  $X_4$ .

(b) Variation of  $X_1 = \gamma_s D^3 / \rho v^2$

Two series of tests were conducted in the wave flume using sand as the sediment. The first series was in cold water at 6°C and the second series was in relatively warm

water at 22°C. The viscosity of the cold water was one and a half times the viscosity of the warm water, thus providing a range in viscosity similar to that normally found under prototype conditions. For the first series of tests  $X_1 = 346.6$  and for the second series of tests  $X_1 = 801.9$ .

There was virtually no difference in bed form length, height or steepness for different values of  $X_1$ . Therefore, assuming a null hypothesis for differences in  $X_1$ , a significance test was applied to the data. For bed form length and height, there was no significant difference at the 5% probability level, between the results for the two values of  $X_1$ . However, for bed form steepness the null hypothesis was rejected as the results showed a significant difference for the two values of  $X_1$ . Therefore, although  $X_1$  may be a significant variable, the difference it causes over a practical range is so small that it may be considered unimportant.

(c) Variation of  $X_3 = \rho_s / \rho$

In previous studies it has been assumed by Yalin (12) and Carstens et al (2), that the density of the sediment particle is important only when associated with the acceleration due to gravity. That is, in the dimensional analysis, only the parameter  $\gamma_s = (\rho_s - \rho) \cdot g$  was used. This assumption is satisfactory for unidirectional flows where accelerations other than gravitational are negligible, but in oscillatory flows, the fluid and therefore the sediment particles are subject to almost continuous acceleration or deceleration. As the acceleration due to gravity is not the only acceleration involved, the density of the sediment cannot be considered to occur only in association with  $g$ , and it must remain as a separate variable  $X_3$ .

Figures 5 and 6 show that bed forms are indeed a function of  $X_3$ . The lighter material (bakelite,  $X_3 = 1.60$ ) produces bed forms which are both longer and higher than those produced by the denser material (sand,  $X_3 = 2.68$ ). Bed form steepness did not appear to be as sensitive to changes in  $X_3$ . These results obtained from wave flume experiments are at a constant value of  $X_2 = 21.9 \times 10^{-6}$ . The effect of varying  $X_3$  is most important at the high values of  $X_2$  occurring for laboratory waves. Low values of  $X_2$  occurred for experiments with large periods of oscillation in both the wave flume and the oscillating water tunnel and for these conditions the effect of the variable  $X_3$  was found to be insignificant.

To determine why the variable  $X_3$  affects the results as it does, the flow conditions at either end of the ranges of  $X_2$  and  $X_4$  were considered. At low values of  $X_4$  and high values of  $X_2$  as occurring mainly in the wave flume, the maximum fluid accelerations are high. Because of these high accelerations there is a substantial phase lag between the sediment particle velocities and the fluid particle velocities, particularly for sediments of high density. Therefore, the distance the fluid can transport the sediment particles is smaller for the denser sediment, and it follows that bed form lengths and heights will also be smaller. Thus,  $X_3$  has a strong effect on bed form. As  $X_4$  increases while  $X_2$  decreases, fluid accelerations become smaller until at values of  $X_4$  occurring in the water tunnel, the phase lag in velocity for the light and dense particles behind the fluid velocity is small in both cases and  $X_3$  has no effect on the properties of the bed forms.

(d) Variation of  $X_2 = \rho D / \gamma_s T^2$

Figures 7 and 8 are results of experiments in the oscillating water tunnel using polystyrene sediment. For bed form length, Fig. 7, the curves all have an initial slope of 1:1 and they appear to stem from a single straight line. In the case of bed form heights in Fig. 8, the rising slopes of the curves for each value of  $X_2$  all have approximately the same steepness and overlap so that a straight line envelope may be drawn to the data at a slope of approximately 1:1. The curve for  $X_2 = 196.3 \times 10^{-6}$  is an exception since its rising slope is much steeper than for the other  $X_2$  curves.

Tests were also conducted in the oscillating water tunnel using sand and bakelite sediments for which much lower values of  $X_2$  were obtained than for the polystyrene. The results for these tests are given in Figs. 9, 10, 11, 12 along with results from wave flume experiments. For  $X_2 = 21.9 \times 10^{-6}$  in Figs. 11 and 12 two sets of results are presented. One was taken in the oscillating water tunnel and the other in the wave flume, while all other experimental conditions were exactly similar. The agreement between the two sets of results was quite close, giving confidence in the use of the two methods for measurement of the same phenomena.

Although the data in Figs. 7, 9 and 11 falls approximately on straight lines, closer examination reveals that each group of points for a specific value of  $X_2$  actually defines a curve or portion of a curve similar to those shown



in Figs. 1 and 2. Each curve for  $X_2$  describing bed form length is slightly offset to the right from the one at the next higher value of  $X_2$ , so that the data as appearing in Figs. 7, 9 and 11 seems to define one straight line at a slope slightly less than 1:1.

The experimental results for the sand and bakelite could not be extended to very high values of  $X_4$  for constant values of  $X_2$ , due to physical limitations of the experimental equipment.

The experimental results showing the effect of variation of  $X_2$  on the bed form steepness, are shown in Figs. 13, and 14. The data obtained using polystyrene clearly shows a series of curves for different values of  $X_2$ . The maximum steepness for a particular value of  $X_2$ , decreases as the value of  $X_2$  increases. Thus, for the high values of  $X_2$  obtained in the wave flume, bed form steepness was approximately 0.14. For the highest value of  $X_2$  obtained, i.e.  $196.3 \times 10^{-6}$ , using polystyrene in the water tunnel, the maximum steepness was 0.115. In Fig. 14 showing bed form steepness in the bakelite experiments, there is more scatter in the data, but in some cases the characteristic rising and falling curves may be distinguished.

#### (e) Design Curves

From the experimental data for bed form length and height presented, it may be seen that for a specified value of  $X_2$  there are maximum possible values of length and height. These maximum values are plotted against  $X_2$  in the Figs. 15 and 16. Included are the results of Carstens et al (2) who also used an oscillating water tunnel. They show a reasonable agreement with the results of the present experiments.

Having obtained the two curves for maximum possible bed form length and height in Figs. 15 and 16, it is possible to plot the design curves for bed form length as in Fig. 17 and for bed form height as in Fig. 18. These curves neglect the effects of  $X_1$  and  $X_3$ . Although neglecting  $X_3$  at the highest values of  $X_2$  may introduce an error of approximately 15%, for  $X_2 < 20 \times 10^{-6}$  the error would be negligible.

Using Figs. 17 and 18 it is now possible to determine the length and height of bed form that will develop on any specified sediment bed for given conditions of fluid

oscillation amplitude and period.

#### CONCLUSIONS

Experiments have been conducted in both a laboratory wave flume and an oscillating water tunnel to determine the characteristics of bed forms produced by wave action. From the results of these experiments the following conclusions are drawn.

1. For the variation of bed form length with  $X_4$ , as  $X_4$  increases, bed form length is initially dependent only on the fluid orbit length. At large values of  $X_4$ , the bed form becomes directly proportional to the grain size diameter. The constant of proportionality is a function of  $X_2$ . Bed form height and steepness at first increase with increasing  $X_4$ , reach maximum values and then decrease until the bed form disappears.
2. Tests conducted over the practical range of viscosity showed that the difference in bed form caused by  $X_1$  is so small as to be unimportant.
3.  $X_3$  was shown to be an important variable as in the present experiments, results for  $X_3 = 2.68$  and  $X_3 = 1.60$  showed a difference of approximately 15% in bed form length and height. However,  $X_3$  is an important variable only at high values of  $X_2$ , i.e. for  $X_2$  greater than approximately  $20 \times 10^{-6}$ .
4. Graphs have been presented to show the variation of bed form length, height and steepness with  $X_2$ . At values of  $X_2$  greater than approximately  $200 \times 10^{-6}$ , bed forms do not appear on a sediment bed.
5. Design curves have been drawn by means of which it is possible to predict the length and height of bed form that will develop on any specified sediment bed for given conditions of fluid oscillation amplitude and period.

#### ACKNOWLEDGEMENTS

The authors are grateful to the National Research Council of Canada for the financial support for this program of study during which the senior author was a Gledden Fellow of the University of Western Australia.

## REFERENCES

1. Bagnold, R.A., "Motion of Waves in Shallow Water. Interaction between Waves and Sand Bottoms". Proc. Roy. Soc. Lond., Series A, Vol. 187, 1946, pp.1-15.
2. Carstens, M.R., Neilson, F.M. and Altinbileck, H.D., "Bed Forms Generated in the Laboratory under an Oscillatory Flow: Analytical and Experimental Study". C.E.R.C., Tech. Memo No. 28, 1969.
3. Homma, M. and Horikawa, K., "Suspended Sediment Due to Wave Action". Proc. 8th Conf. on Coastal Eng., Mexico City, 1962, pp.168-193.
4. Horikawa, K. and Watanabe, A., "A Study on Sand Movement Due to Wave Action". Coastal Eng. in Japan, Vol. 10, 1967, pp.39-57.
5. Inman, D.L., "Wave Generated Ripples in Nearshore Sands". Beach Erosion Board, Tech. Memo 100, 1957.
6. Kennedy, J.F. and Falcon, M., "Wave Generated Sediment Ripples". M.I.T. Hydrodynamics Lab. Rep. No. 86, 1965.
7. Manohar, M., "Mechanics of Bottom Sediment Movement Due to Wave Action". Beach Erosion Board, Tech. Memo 75, 1955.
8. Riedel, H.P., "Direct Measurement of Bed Shear Stress Under Waves". Ph.D. Thesis, Queen's University at Kingston, 1972.
9. Scott, T. "Sand Movement by Waves". Beach Erosion Board, Tech. Memo 48, 1954.
10. Silvester, R., "Modelling of Sediment Motions Offshore". Jr. of Hyd. Res., I.A.H.R., Vol. 8, No. 2, 1970, pp.229-259.
11. Yalin, M.S., "Mechanics of Sediment Transport". Pergamon Press, 1972 (in press).
12. Yalin, M.S. and Russell, R.C.H., "Similarity in Sediment Transport Due to Waves". Proc. 8th Conf. on Coastal Eng., Mexico City, 1962, pp.151-167.

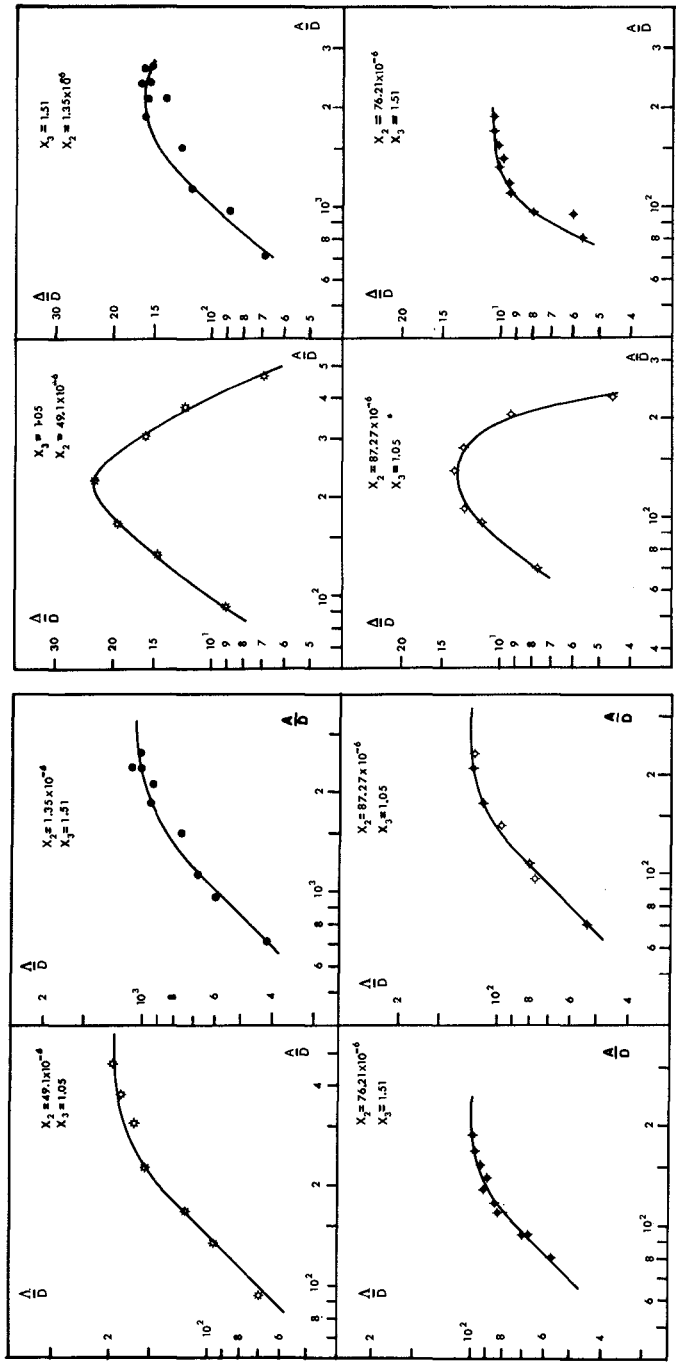


FIG.2 VARIATION OF  $\Delta/D$  WITH  $X_4 = A/D$

FIG.1 VARIATION OF  $\Delta/D$  WITH  $X_4 = A/D$

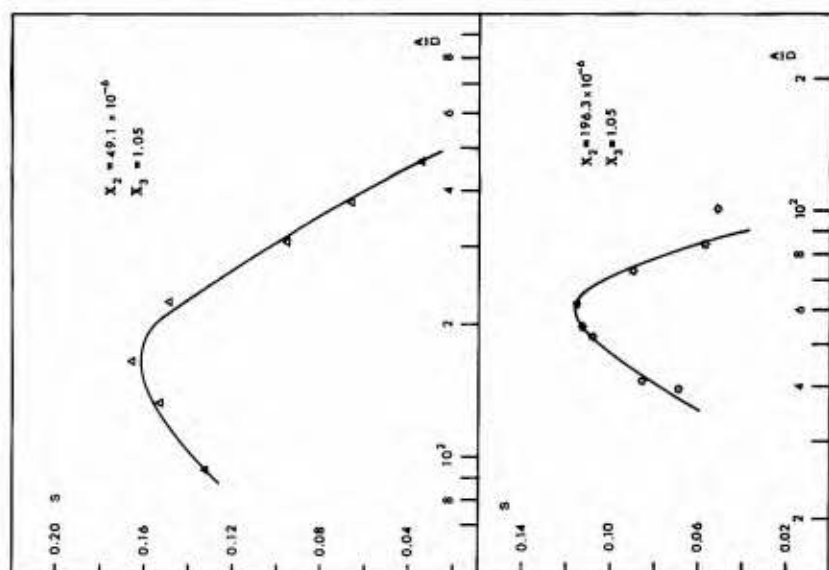


FIG. 4 THE OSCILLATING WATER TUNNEL

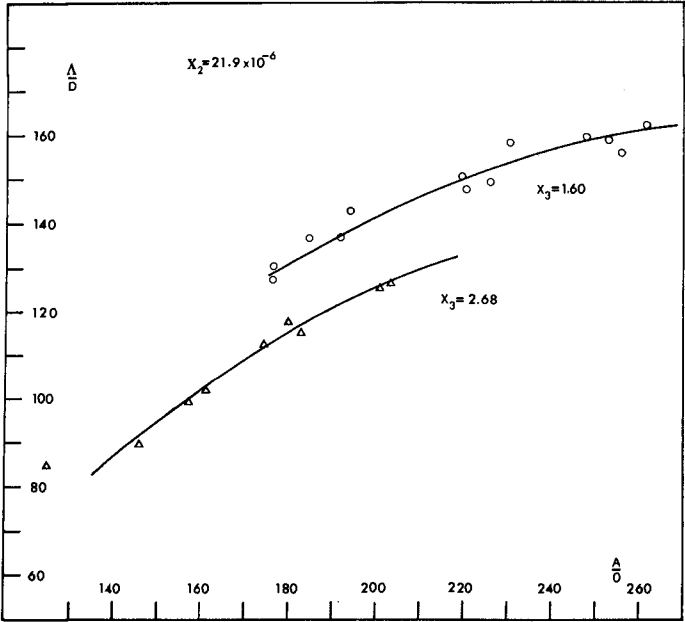


FIG.5 VARIATION OF  $\Delta/D$  WITH  $X_3 = \rho_3/\rho$

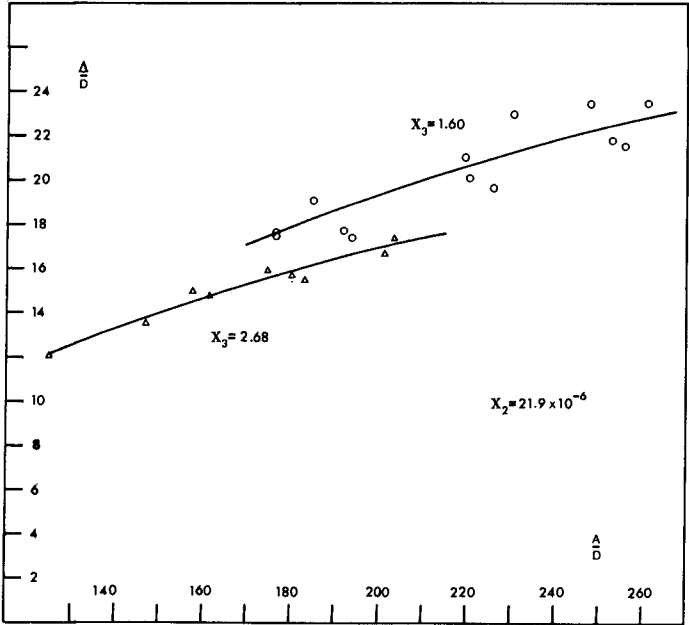
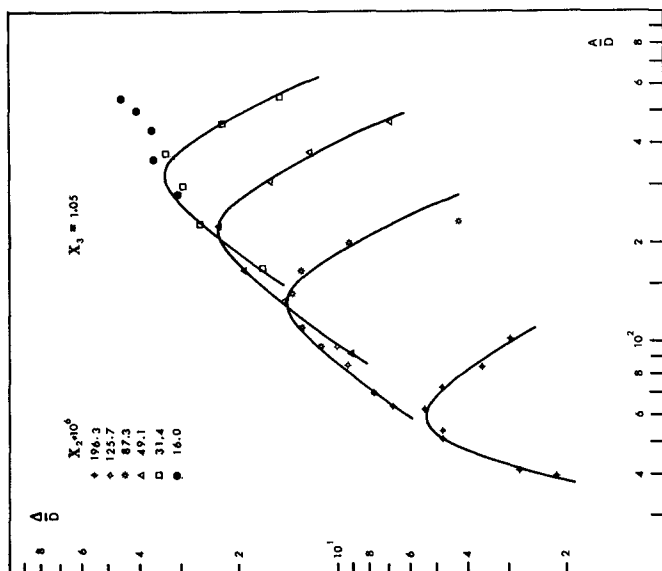
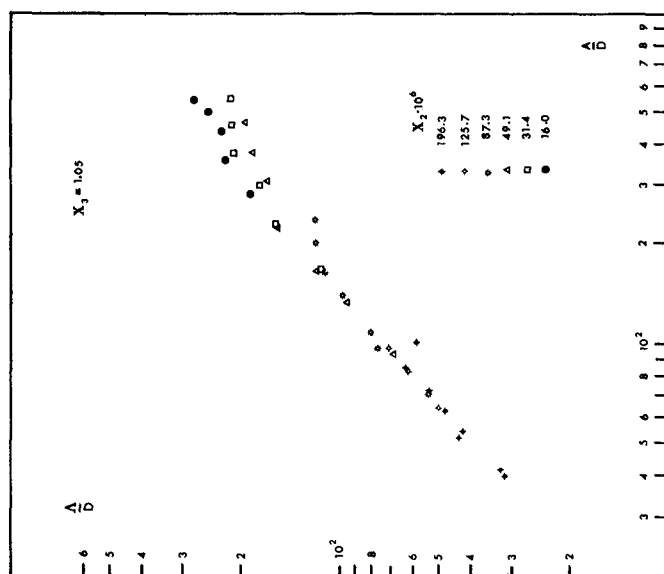


FIG.6 VARIATION OF  $\Delta/D$  WITH  $X_3 = \rho_3/\rho$

FIG. 8 VARIATION OF  $\Delta/D$  WITH  $X_2 = \rho D / \gamma_s T^2$  (POLYSTYRENE)FIG. 7 VARIATION OF  $\Delta/D$  WITH  $X_2 = \rho D / \gamma_s T^2$  (POLYSTYRENE)

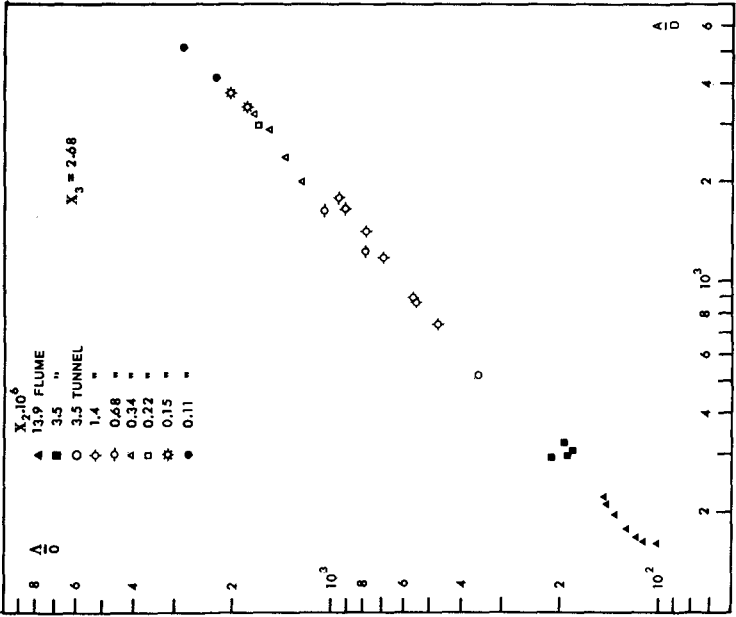
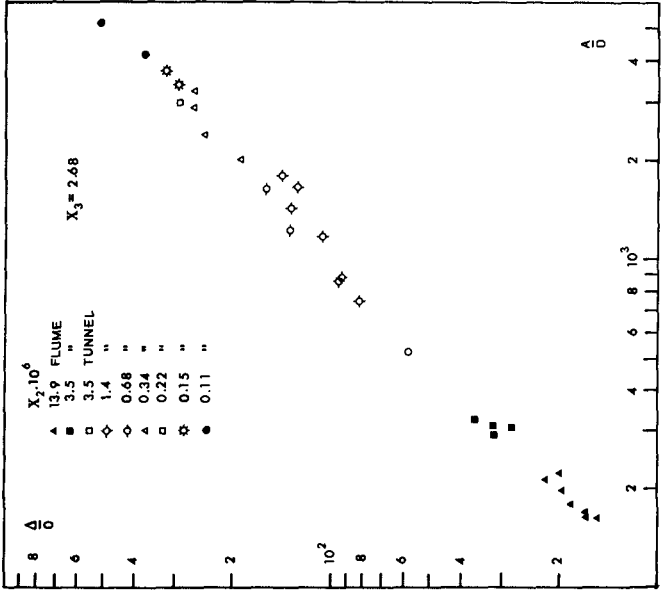


FIG.10 VARIATION OF  $\Delta/D$  WITH  $X_2 = \rho D / \gamma_s T^2$  (SAND)





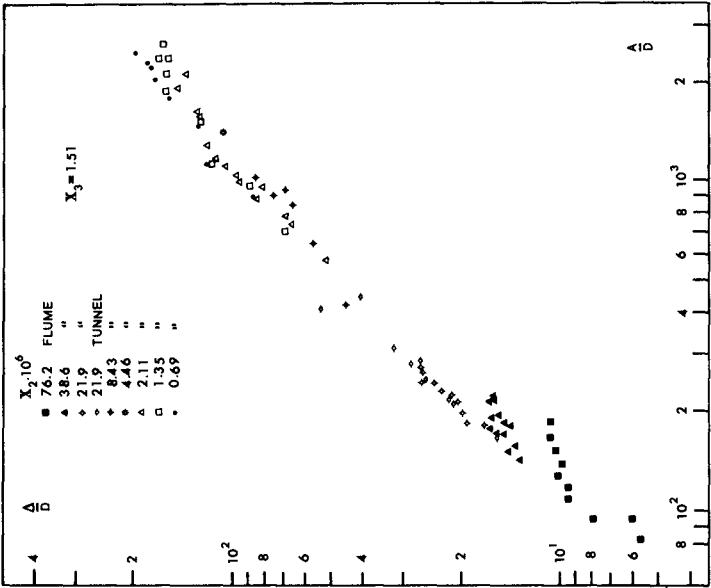


FIG.12 VARIATION OF  $\Delta/D$  WITH  $X_2 = \rho D / \gamma_s T^2$   
(BAKELITE)

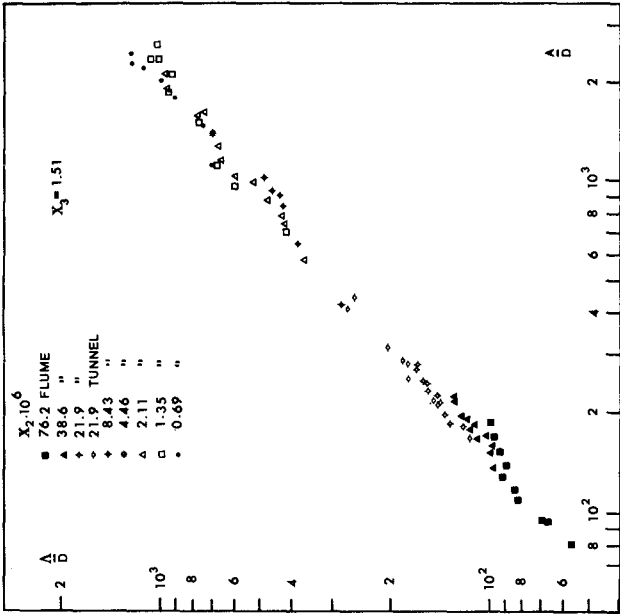


FIG.11 VARIATION OF  $\Delta/D$  WITH  $X_2 = \rho D / \gamma_s T^2$   
(BAKELITE)

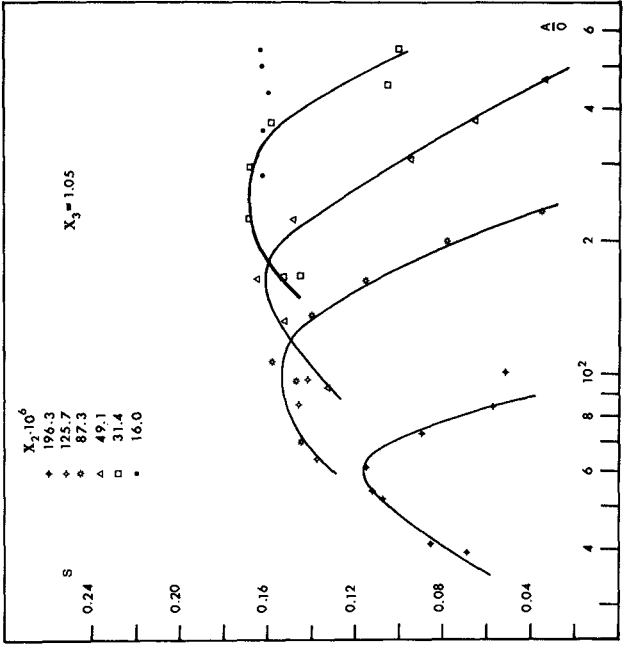


FIG.13 VARIATION OF S WITH  $X_2 = \rho D / \gamma_s T^2$   
(POLYSTYRENE)

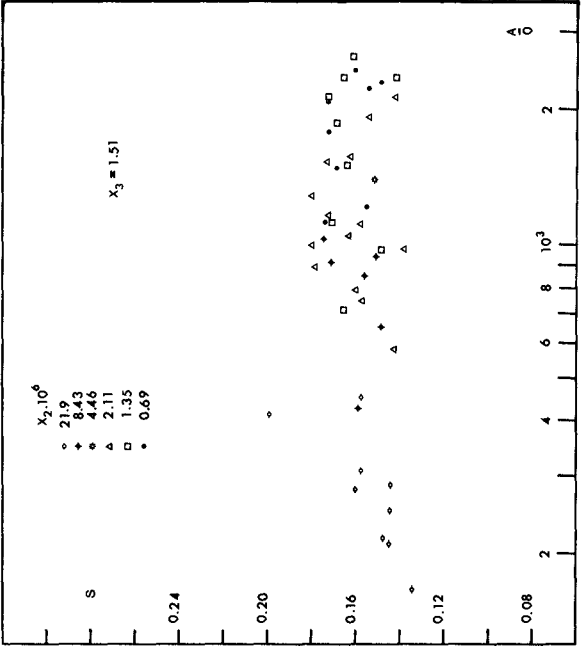


FIG.14 VARIATION OF S WITH  $X_2 = \rho D / \gamma_s T^2$   
(BAKELITE)

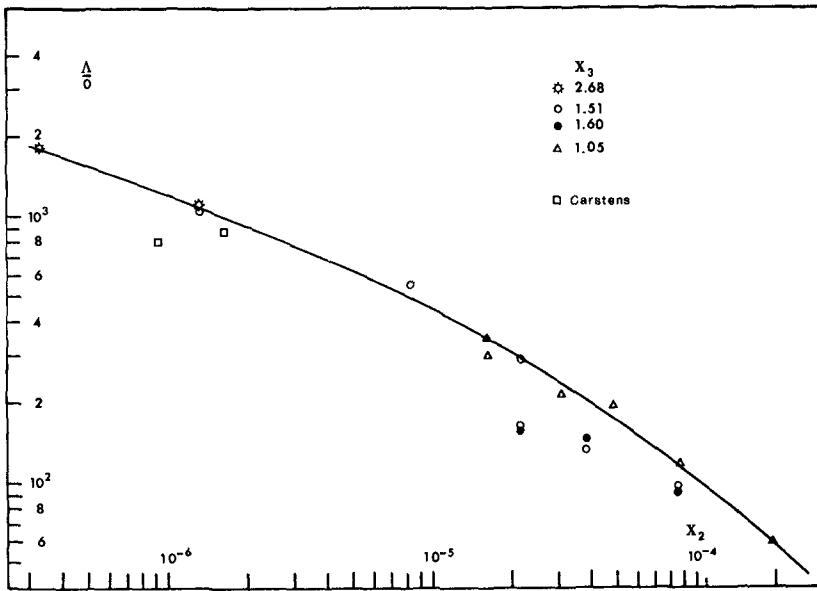


FIG.15 MAXIMUM POSSIBLE  $\Delta/D$

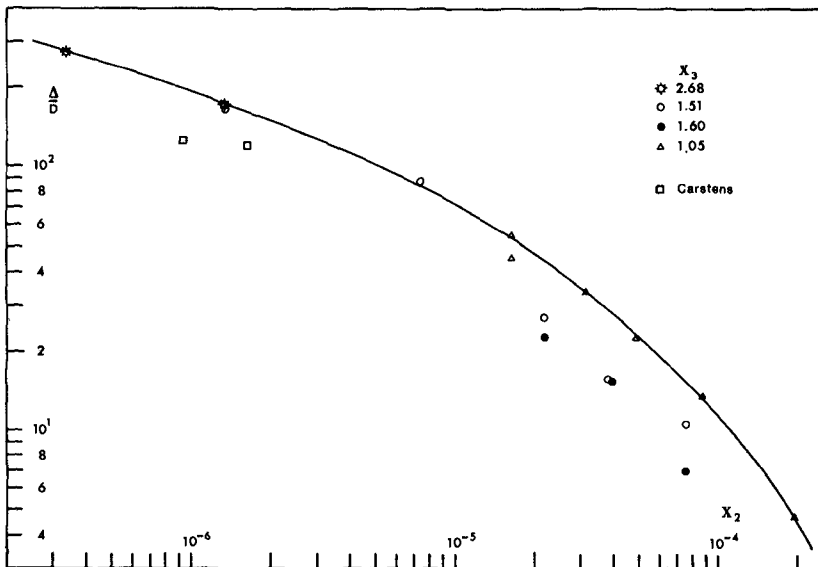


FIG.16 MAXIMUM POSSIBLE  $\Delta/D$

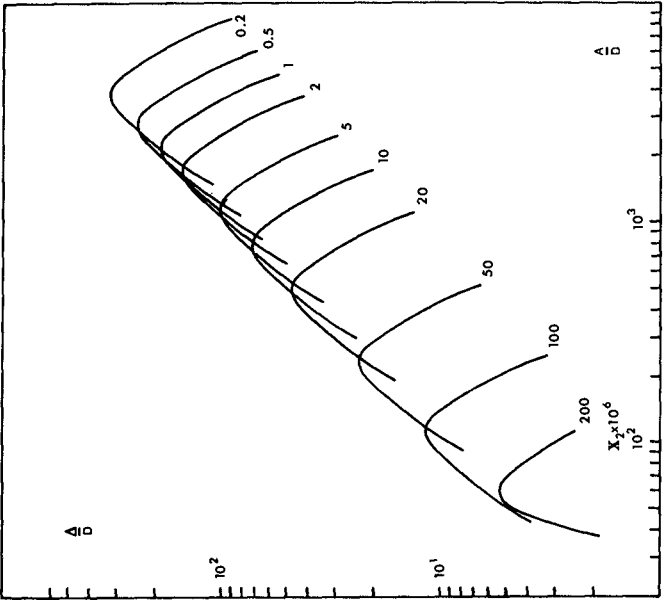


FIG.18 DESIGN CURVES FOR BED FORM HEIGHT

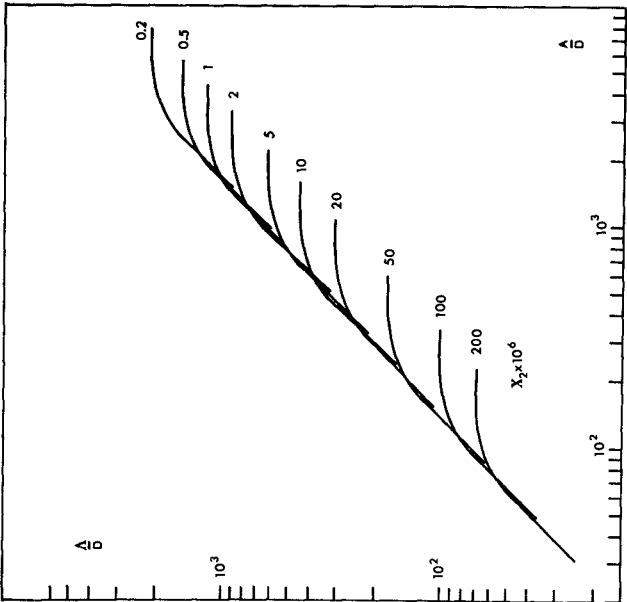


FIG.17 DESIGN CURVES FOR BED FORM LENGTH